Bulk-to-Surface Proton-Coupled Electron Transfer Reactivity of the Metal-Organic Framework MIL-125

Caroline T. Saouma,*[,‡,∞] Sarah Richard,[‡,†] Simon Smolders,[ℓ] Murielle F. Delley,[δ] Rob Ameloot,[ℓ] Frederik Vermoortele,[ℓ] Dirk E. De Vos,*[,ℓ] James M. Mayer*[,‡,δ]

[‡] Department of Chemistry, University of Washington, Box 351700, Seattle, Washington 98195-1700, U.S.A.

[∞] Department of Chemistry, University of Utah, 315 S 1400 E, Salt Lake City, Utah, 84112-0850, U.S.A.

[δ] Department of Chemistry, Yale University, PO Box 208107, New Haven, Connecticut, 06520-8107, U.S.A.

[ℓ] Centre for Surface Chemistry and Catalysis, KU Leuven – University of Leuven, Celestijnenlaan 200F p.o. box 2461, 3001 Leuven, Belgium

ABSTRACT: Stoichiometric proton-coupled electron transfer (PCET) reactions of the metal-organic framework (MOF) MIL-125, $Ti_8O_8(OH)_4(bdc)_6$ (bdc = terephthalate) are described. In the presence of UV-light and isopropanol, MIL-125 was photo-reduced to a maximum of 2(e^- + H^+) per Ti_8 node. This stoichiometry was shown by subsequent titration of the photo-reduced material with the 2,4,6-tri-*t*-butylphenoxyl radical. This reaction occurred by PCET to give the corresponding phenol and the original, oxidized MOF. The high level of charging, and the independence of charging amount with particle size of the MOF samples, shows that the MOF was photocharged throughout the bulk and not only at the surface. NMR studies showed that the product phenol is too large to fit in the pores, so the phenoxyl reaction must have occurred at the surface. Attempts to oxidize photo-reduced MIL-125 with pure electron acceptors resulted in multiple products, underscoring the importance of removing e^- and H^+ together. Our results require that the e^- and H^+ stored within the MOF architecture must both be mobile, to transfer to the surface for reaction. Analogous studies on the soluble cluster $Ti_8O_8(OOC^tBu)_{16}$ support the notion that reduction occurs at the Ti_8 MOF nodes and furthermore that this reduction occurs via e^-/H^+ (H-atom) equivalents. The soluble cluster also suggests degradation pathways for the MOFs under extended irradiation. The methods described are a facile characterization technique to study redox-active materials and should be broadly applicable to, for example, porous materials like MOFs.

Supporting Information Placeholder

Introduction

Metal-organic frameworks (MOFs) are emerging as promising materials for facilitating redox reactions, including multi-e^-/multi-H^+ transformations. Recent studies highlight the ability of the organic linkers or metal ions in or on the MOF nodes to undergo 1-e^- oxidations,[1–4] for the MOFs themselves to serve as conductive materials[5–7] or semiconductors,[8,9] and for the MOFs to facilitate redox reactions that are pertinent to fuel cells and energy.[10–12] In this latter context, the development of MOF photocatalysts that mimic the reactivity of bulk TiO_2 is of timely interest.[13–19]

Common photocatalytic reactions such as water splitting or CO_2 reduction are fundamentally proton-coupled electron transfer (PCET) processes. Therefore, tuning the PCET properties of the catalyst is of the utmost importance.[20–22] In this context, several groups have developed MOFs that show PCET behavior resulting in good photo-and electrochemical activities.[22–24] PCET has been suggested to occur on the linker,[24] the node[25] and on the linker and node combined[22,23] but has not been studied in well-known photoactive MOFs. In this work, we provide an in-depth analysis of the PCET behavior in the widely used MIL-125.

The Ti-based MOFs MIL-125[16] ($Ti_8O_8(OH)_4(bdc)_6$) and NH_2-MIL-125[13] ($Ti_8O_8(OH)_4(bdc\text{-}NH_2)_6$) (bdc-$NH_2$ = 2-aminoterephthalate) have planar Ti_8 nodes with oxide and hydroxide ligands, linked with terephthalate (bdc) groups. These materials have been shown to be photo-active; for instance UV irradiation of a slurry of MIL-125 in benzyl alcohol formed benzaldehyde with a color change to blue.[16] It was suggested that this process reduces each MOF node (Ti_8 cluster) by a net H-atom (eq 1). Though the stoichiometry of the reduction was not established, the proposed eq 1 led us to hypothesize that the reduced MOF should be able to facilitate well-defined PCET reactions.

$$Ti_8O_8(OH)_4(bdc)_6 + 0.5\ PhCH_2OH \xrightarrow{h\nu} Ti_7Ti^{III}O_7(OH)(OH)_4(bdc)_6 + 0.5\ PhCHO \quad (1)$$

NH_2-MIL-125 can be reduced by *visible* light in the presence of a sacrificial reductant, which is highly desirable for photocatalysts.[13] In the presence of triethanolamine (TEOA), visible light irradiation of NH_2-MIL-125 results in the catalytic reduction of nitrobenzene to aniline,[15] CO_2 to formate,[13] and protons (aq) to H_2.[14,15,26]

Herein we describe fundamental studies of MIL-125 that address basic mechanistic questions associated with MOF photocatalysis, such as whether the redox chemistry takes place only at the surface of the MOF particles or occurs throughout the pores. Specifically, we develop a solution NMR assay to determine the reduction stoichiometry, the number of e^- + H^+ (H atoms) transferred per node. We show by judicious choice of substrates that MIL-125 can undergo well-defined PCET reactions. The results

show that irradiation causes reduction throughout the MOF, but all of the (e^- + H^+) can be removed through PCET reactions that occur only at the surface. This work thus develops our understanding of the redox capabilities in MOFs, which should advance the promising area of using MOF materials to facilitate multi-e^-/multi-H^+ transformations.

Results and Discussion

I. PCET Chemistry of the MOF MIL-125

Irradiation of MIL-125 in neat ^{i}PrOH results in a color change from white to dark blue, indicating reduction of the MOF. The EPR spectrum of this material is similar to that reported for photo-reduction with benzyl alcohol and exhibits overlapping broad EPR resonances at ca. g = ca. 1.94 (see SI)[16] Quantification of the radical yield has not been attempted due to the non-trivial nature of the signal. The reduced MOF can be isolated and stored as a solid in the glovebox for days with little decay in the absence of oxygen. Re-suspension of the reduced material in C_6D_6 and addition of 2,4,6-tri-*t*-butyl-phenoxyl radical (^{t}Bu$_3$ArO$^\bullet$) or the nitroxyl radical 2,2,6,6-tetramethyl-1-piperidinyloxy (TEMPO) resulted in a color change back to white over ~30 min, indicative of oxidation of the reduced MOF. ^{1}H NMR spectra of ^{t}Bu$_3$ArO$^\bullet$ reactions showed exclusive formation of ^{t}Bu$_3$ArOH, indicative of a net PCET reaction (H-atom transfer reaction) (eq 2). No ^{t}Bu$_3$ArO$^-$ was observed, which would have suggested pure electron transfer (ET) from the reduced MOF. Thus, the photo-reduced MIL-125 is capable of facilitating PCET.

$$Ti_{8-x}Ti^{III}{}_xO_{8-x}(OH)_{4+x}(bdc)_6 + x\ {}^tBu_3ArO^\bullet \longrightarrow Ti_8O_8(OH)_4(bdc)_6 + x\ {}^tBu_3ArOH \quad (2)$$

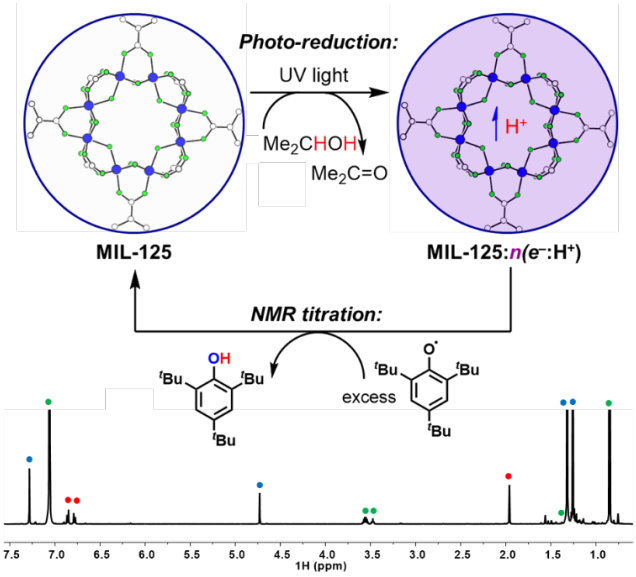

Figure 1. (top): Scheme showing the photo-reduction of MIL-125 and subsequent oxidation. For simplicity, only one Ti_8 cluster is shown (the structure of MIL-125 is depicted within the blue circles). For maximum photo-reduction, n ≅ 2. (bottom): ^{1}H NMR spectrum of the subsequent reaction with ^{t}Bu$_3$ArO• (C_6D_6). The colored dots identify ^{t}Bu$_3$ArOH (blue), Ar_2O (internal standard, red), and C_6D_5H, THF, ^{i}PrOH (green).

To determine the stoichiometry and extent of reduction, a simple solution ^{1}H NMR method was developed to quantify the e^-/H^+ equivalents transferred to MIL-125. This method uses ^{1}H NMR quantification of a redox probe relative to an internal standard. After photo-reduction, the MOF was isolated as a solid in the glovebox. A known weight was re-suspended in C_6D_6 and a calibrated C_6D_6 solution of ^{t}Bu$_3$ArO$^\bullet$ and di-*p*-tolyl-ether (Ar_2O) was added. The suspension was stirred for at least 3.5 h to ensure complete oxidation of the MOF. ^{1}H integration of ^{t}Bu$_3$ArOH *vs.* the Ar_2O standard provided quantification of the reducing equivalents transferred (Figure 1).

For accurate NMR integration, it is essential that neither the internal standard nor the redox probe bind to or be taken up in the MOF, as this would diminish the observed concentration. Addition of MIL-125 or photo-reduced MIL-125 to NMR samples containing ^{t}Bu$_3$ArOH and Ar_2O does not change the relative integration of the two species, indicating that neither was adsorbed (see SI). Given the similarity in size and charge between ^{t}Bu$_3$ArO$^\bullet$ and ^{t}Bu$_3$ArOH, it is very likely that the radical oxidant likewise is not taken up into the pores. By contrast, TEMPOH was shown to be taken up by MIL-125, precluding the use of TEMPO$^\bullet$ as a redox probe (see SI).

Several suspensions of MIL-125 in ^{i}PrOH were irradiated for various amounts of time and analyzed by titration with ^{t}Bu$_3$ArO$^\bullet$. A plot of H-atom equivalents transferred per Ti_8 node versus photolysis time (Figure 2) shows that increasing the photolysis time increases the extent of reduction. Since EPR spectra indicate that reduction occurs at Ti,[16] we report the number of reducing equivalents relative to the Ti_8 nodes (the moles of Ti_8 nodes was determined from the mass of the MOF, and the moles of H-atoms transferred from the NMR method). The increased reduction with time was also evident by eye, as the blue color of the MOF suspension became darker with longer irradiation time. After 5 h, each Ti_8 node is reduced by at least 0.4 H-atoms. At long irradiation times, MIL-125 can be reduced by up to 2 H-atom equivalents per Ti_8 cluster.

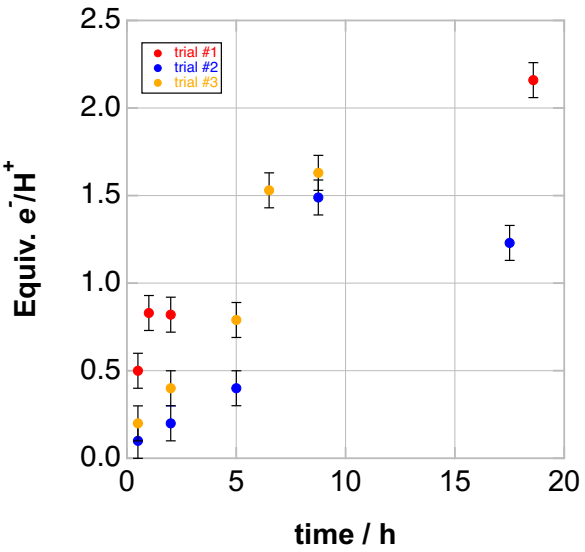

Figure 2. Number of reducing equiv. per Ti_8 node vs. time for three different photo-reductions of MIL-125 using a 200 W Hg/Xe lamp. Errors for data points are estimated to be ≤ ± 0.1 equiv. e^-/H^+, based on the error of NMR analysis by integration also taking into account error propagation from the balance accuracy and the estimated maximal sample loss. The sample in trial #2 (blue circles) became black by 17.5 h of photolysis and the color persisted after addition of excess ^{t}Bu$_3$ArO$^\bullet$, indicating decomposition.

The variability in extent of reduction between the three experiments was attributed to differences in the irradiation conditions,

such as distance from lamp, stirring rate and nature of the suspension, solvent volume, type of quartz vessel, and beam focus (see SI). In some instances, prolonged irradiation gave fewer H-atom equivalents than anticipated (Figure 2), which is attributed to MOF degradation (*vide infra*).

To test that the irradiation did not degrade the MOF, two types of experiments were done on various samples. In the first, powder XRD was collected on the photo-reduced MOF material. The X-ray diffraction patterns showed no loss in crystallinity of the material upon photo-reduction, and no new reflections were observed (see SI). The second experiment used ^{1}H NMR analysis of material formed after titration with ^{t}Bu$_3$ArOH. After removal of the C_6D_6 solvent and re-suspension in d_7-DMF, the ^{1}H NMR spectrum only showed resonances attributed to solvent, Ar_2O, and ^{t}Bu$_3$ArOH. No terephthalic acid or soluble terephthalate species were detected in the samples in which the titration restored the white color of the oxidized MOF. By contrast, terephthalic acid was present in the solution that corresponds to the blue point at 17.5 h in Figure 2, for which the dark color persisted after oxidation. These observations are indicative of MOF degradation, and suggest that extended UV-irradiation may degrade MIL-125 under certain conditions.

The measured stoichiometries show that the photo-reductions must be reducing the Ti_8 clusters throughout the MOF particles, not only at the surface. The fraction of Ti_8 nodes that are at the surface was estimated using the roughly elliptical morphologies of the MIL-125 particles observed by SEM, with semi-axes that range from 300 (± 100) to 850 (± 50) nm (SI). Assuming perfect ellipsoids, the volumetric fraction of the outermost shell – one layer of Ti_8 nodes and linker, 1.9 nm – contains only 1.3 % of the Ti_8 clusters. If reduction occurred exclusively in this outer-shell, then each surface Ti_8 cluster would have to be reduced by ~88 H-atoms, or ~11 H-atoms for each Ti atom, to achieve the observed 1 e^-/H$^+$ per Ti_8 cluster throughout the MOF. Studies with different batches of MIL-125 that differ in size and morphology, ranging from spheres with 85 nm radii to truncated octahedra with radii of 2650 nm, all showed facile reduction to 1 e^-/H$^+$ per bulk Ti_8 cluster. All of these results would require unrealistically high numbers of e^-/H$^+$ per surface Ti (see SI). Thus, both the Ti_8 nodes at the surface and within the MOF must have been reduced.

The above studies indicate photo-reduced MIL-125 can transfer net H-atom equivalents ($e^- + H^+$) to ^{t}Bu$_3$ArO$^\bullet$. It is also possible to remove some of the electrons with the simple outer-sphere oxidant decamethylferrocenium hexafluorophosphate ([FeCp$^*_2{}^+$]PF$_6^-$). Treatment of reduced MIL-125 with [FeCp$^*_2{}^+$]PF$_6^-$ resulted in some lightening of the blue color and ^{1}H NMR analysis showed the presence of both FeCp$^*_2{}^+$/FeCp$^*_2$, indicative of oxidation of the MOF solid. (FeCp$^*_2$ does not fit in the pores of MIL-125 or photo-reduced MIL-125, see SI). As FeCp$^*_2{}^+$ and FeCp$^*_2$ undergo fast electron exchange on the NMR timescale, a single resonance for the two species is observed. The position of this resonance indicates the mole fractions (χ) of the two species (eq 3).[27]

$$\delta_{obs} = \chi_{FeCp^*2}\,\delta_{FeCp^*2} + \chi_{FeCp^*2+}\,\delta_{FeCp^*2+} \qquad (3)$$

Identical samples of reduced MIL-125 transferred fewer reducing equivalents to FeCp$^*_2{}^+$ (electron transfer, ET) than to ^{t}Bu$_3$ArO$^\bullet$ (PCET/H-atom transfer). In one comparison, FeCp$^*_2{}^+$ removed 0.36 e^- versus 0.83 H-atom equivalents per Ti_8 node by ^{t}Bu$_3$ArO$^\bullet$. Further, the resulting solution NMR spectrum of MIL-125 that has been treated with FeCp$^*_2$ had several new, unidentifiable resonances, indicative of side reactions. Attempts to use other oxidants, including anilinium radicals, likewise did not give clean electron-transfer chemistry. Thus, PCET seems to be more facile and reversible chemistry for the MOF than simple ET. The advantage of chemical reactions that move electrons and protons together is that charge balance is maintained. A principle of solid state chemistry is that each unit cell must be electrically neutral, and that should apply to MOF materials as well. Removal of just electrons from the MOF leaves an unfavorable positive charge, which likely makes the remaining protons more acidic and leads to decay of the MOF.

The PCET reaction with ^{t}Bu$_3$ArO$^\bullet$ must occur at the surface because ^{t}Bu$_3$ArOH is too large to enter the MOF pores (see above). Since complete re-oxidation is observed, the e^-/H$^+$ equivalents must be able to migrate through the MOF to the surface. Thus, the material allows for e^-/H$^+$ hopping. Proton[28–31] and electron[5–7] conductivity in MOFs have already been described; in this study, the two occur together here to maintain charge balance (see above). The proton migration likely occurs via trapped alcohol in the MOF pores and through mobility of the H$^+$ from the clusters' bridging hydroxides, a process very similar to that observed in Zr-based MOFs.[32,33] The H$^+$ ion accompanying the e$^-$ will likely bind to a bridging oxygen on the MIL-125 cluster to form a hydroxide. A similar mechanism has been shown for COK-69, another photo-reducible Ti-MOF.[25] Similarly, the PCET reduction of bulk TiO_2 and other oxides is thought to form hydroxides.[34] Broad EPR resonances at RT for reduced MIL-125 have previously been ascribed to e^- hopping between different Ti centers.[16] The e^-/H$^+$ hopping mechanism between different Ti_8 nodes is not clear. The kinetics of this process are likely complicated and multi-exponential due to the size dispersion of the MIL-125 crystals. Monitoring the time course of the formation of ^{t}Bu$_3$ArOH from reaction of photo-reduced MIL-125 with ^{t}Bu$_3$ArO$^\bullet$ over time is consistent with multi-exponential kinetics and shows that the reaction is complete within 30-60 min (SI).

II. PCET Chemistry of the soluble cluster $Ti_8O_8(OOC^tBu)_{16}$

Parallel studies using a known, well-defined molecular cluster, $Ti_8O_8(OOC^tBu)_{16}$ (**Ti$_8$**),[35] provide additional insight into the nature of the photo-reduced state and possible degradation pathways. Cluster **Ti$_8$** serves as a model for the nodes of MIL-125, with a similar ring of eight Ti atoms that are connected via bridging oxo ligands in a relatively flat arrangement (Figure 3). The ligand arrangement differs from that in MIL-125 in that the MOF has four fewer bridging carboxylates decorating the outside of the ring and an additional four bridging hydroxo ligands in the interior of the ring. The empirical cluster formula in the MOF is $Ti_8O_8(OH)_4(OOCR)_{12}$ (Figure 1) vs. the molecular $Ti_8O_8(OOC^tBu)_{16}$. We chose the **Ti$_8$** cluster with alkyl carboxylates rather than the related benzoate that is more analogous to MIL-125 because of the limited solubility and uninformative ^{1}H NMR spectrum of $Ti_8O_8(OOCPh)_{16}$. **Ti$_8$** is readily identified by its two sharp ^{1}H NMR resonances at 1.28 and 1.37 (C_6D_6) that correspond to ^{t}Bu groups that are axial and equatorial with respect to the planar Ti_8 ring.

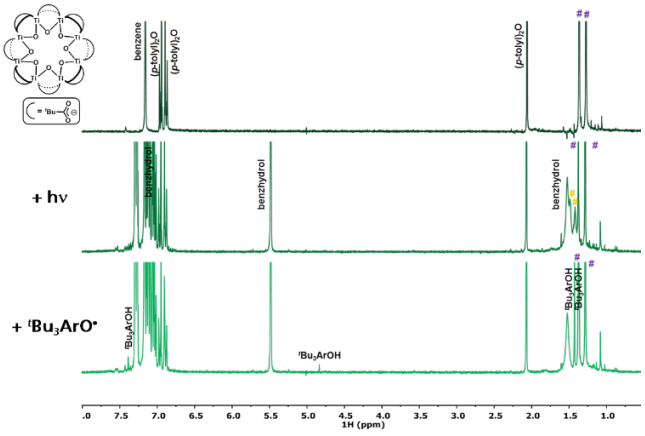

Figure 3. ^{1}H NMR spectra (C_6D_6, 500 MHz): (top): **Ti$_8$** with Ar_2O standard; (middle): after 15 min of irradiation with excess benzhydrol; (bottom): after addition of ^{t}Bu$_3$ArO$^\bullet$. Peaks marked with purple # correspond to **Ti$_8$**, whilst orange # correspond to the speculative H-atom reduced cluster.

Irradiation of a C_6D_6 solution of **Ti$_8$** (0.95 mM), benzhydrol (Ph_2CHOH, 45 mM) and Ar_2O internal standard for 15 min resulted in darkening of the solution to blue. The ^{1}H NMR spectrum of this reaction revealed the presence of two broad new resonances at 1.41 and 1.48 ppm, along with the presence of unreacted **Ti$_8$** (Figure 3). Integration showed 80 % of starting **Ti$_8$** accounted for, and of this material, ~ 43% has been converted to the new species. Treatment of this solution with 1 equiv of ^{t}Bu$_3$ArO$^\bullet$ caused an immediate color change from blue to pale grey. The ^{1}H NMR spectrum of this solution shows the single set of ^{t}Bu resonances of **Ti$_8$** (85% mass balance from initial mass), and resonances ascribed to ^{t}Bu$_3$ArOH (64% yield by initial mass). These results suggest that the new resonances correspond to a photo-reduced cluster. Its reactivity with ^{t}Bu$_3$ArO$^\bullet$ suggests that the new cluster has been reduced by 1e^- and 1H$^+$.

The observation of only two ^{t}Bu resonances for the reduced cluster indicates that this cluster retains the effective 8-fold symmetry of the ring on the NMR timescale. This suggests that the proton is moving around the Ti_8 ring rapidly on the NMR timescale. Such rapid proton movement is consistent with the proton movement during oxidation of the reduced MIL-125.

The discrepancies in mass balance in the **Ti$_8$** chemistry indicate that partial cluster degradation accompanies photo-reduction, and that some of the NMR silent Ti^{III} species can reduce ^{t}Bu$_3$ArO$^\bullet$ (see SI for UV-vis studies). Increasing the irradiation time gave rise to several additional resonances in the corresponding ^{1}H NMR spectrum, indicative of multiple reduction products. Similar results are noted when pivalic acid is added as a sacrificial reductant. Resonances that correspond to pivalic acid, isobutane, and isobutene implicate the intermediacy of ^{t}Bu$^\bullet$, which disproportionates to the hydrocarbon products. Thus, the carboxylate ligands of **Ti$_8$** can serve as a sacrificial reductant (photo-reduction also occurs in the absence of an added alcohol). A similar process has been reported for pivalate on single crystal TiO_2 surfaces.[36] The reduced **Ti$_8$** cluster reacts much more rapidly with ^{t}Bu$_3$ArO$^\bullet$ than the MOF does (≤ seconds vs. hours). This likely reflects the requirement that e^- and H$^+$ diffuse to the surface of the MOF to react with ^{t}Bu$_3$ArO$^\bullet$.

Conclusions

In summary, the proton-coupled electron transfer (PCET) chemistry of MIL-125 has been developed. Irradiation of MIL-125 with ^{i}PrOH as a sacrificial reductant gives a maximum of two (e^- + H$^+$) per Ti_8 cluster node. Subsequent oxidation by ^{t}Bu$_3$ArO$^\bullet$ occurs by PCET to give ^{t}Bu$_3$ArOH. The extent of reduction of the MOF shows that the reducing equivalents must be stored within the MOF and not only on the outer surface. Since ^{t}Bu$_3$ArO$^\bullet$ is too large to enter the MOF, the PCET oxidation must, however, occur at the surface, with the e^- and H$^+$ diffusing from the bulk to the surface. The coupling of e^- and H$^+$ in the MOF likely results from the requirement for charge balance, that it is energetically unfavorable for charges to build up inside the MOF. This study thus presents an unusually detailed look at PCET involving a MOF material. Though there are currently very few well-defined examples, we believe that PCET will prove to be a very common type of redox reactivity in MOFs and other porous materials. This work may therefore be relevant to a number of emerging MOF-applications, such as CO_2 reduction and water splitting. Our results also show the utility of the simple solution NMR methods developed for quantification of e^-/H$^+$ equivalents transferred to the MOF. These methods should be widely applicable to other redox-active MOFs and heterogeneous materials, showing that they can store redox equivalents and that reactivity can be limited to the surface.

ASSOCIATED CONTENT

Supporting Information

Supplementary Information (SI) available (.pdf): Experimental procedures, including NMR spectra, SEM images, and powder XRD plots. The Supporting Information is available free of charge on the ACS Publications website.

AUTHOR INFORMATION

Corresponding Authors

*caroline.saouma@utah.edu
*dirk.devos@kuleuven.be
*james.mayer@yale.edu

Present Addresses

† Laboratoire de Chimie et de Biochimie Pharmacologiques et Toxicologiques, Sorbonne Paris Cité, Université Paris Descartes, CNRS UMR 8601, 45 Rue des Saints Pères, 75006 Paris, France.

Notes

The authors declare no competing financial interests.

ACKNOWLEDGMENT

C.T.S. acknowledges financial support from the U.S. National Institute of Health for postdoctoral fellowship 1F32GM099316. M.F.D. thanks the Swiss National Science Foundation (SNF) for financial support. J.M.M. acknowledges support from the U.S. National Science Foundation awards CHE-1151726 and CHE-1609434. S.S. and D.D.V. gratefully acknowledge the FWO (Aspirant grant and project funding) and KUL Methusalem for funding.

REFERENCES

(1) Brozek, C. K.; Dincă, M. Ti^{3+}-, V$^{2+/3+}$-, Cr$^{2+/3+}$-, Mn^{2+}-, and Fe^{2+}-Substituted MOF-5 and Redox Reactivity in Cr- and Fe-MOF-5. *J. Am. Chem. Soc.* **2013**, *135*, 12886–12891.

(2) Cozzolino, A. F.; Brozek, C. K.; Palmer, R. D.; Yano, J.; Li, M.; Dincă, M. Ligand Redox Non-Innocence in the Stoichiometric Oxidation of Mn_2(2,5-Dioxidoterephthalate) (Mn-MOF-74). *J. Am. Chem. Soc.* **2014**, *136*, 3334–3337.

(3) Smolders, S.; Lomachenko, K. A.; Bueken, B.; Struyf, A.; Bugaev, A. L.; Atzori, C.; Stock, N.; Lamberti, C.; Roeffaers, M. B. J.; De Vos, D. E. Unravelling the Redox-Catalytic Behavior of Ce^{4+} Metal–Organic Frameworks by X-Ray Absorption Spectroscopy. *ChemPhysChem* **2017**, *19*, 373–378.

(4) Su, J.; Yuan, S.; Wang, H.-Y.; Huang, L.; Ge, J.-Y.; Joseph, E.; Qin, J.; Cagin, T.; Zuo, J.-L.; Zhou, H.-C. Redox-Switchable Breathing Behavior in Tetrathiafulvalene-Based Metal–organic Frameworks. *Nat. Commun.* **2017**, *8*, 2008.

(5) Sun, L.; Campbell, M. G.; Dincă, M. Electrically Conductive Porous Metal–Organic Frameworks. *Angew. Chemie Int. Ed.* **2016**, *55*, 3566–3579.

(6) Sheberla, D.; Bachman, J. C.; Elias, J. S.; Sun, C.-J.; Shao-Horn, Y.; Dincă, M. Conductive MOF Electrodes for Stable Supercapacitors with High Areal Capacitance. *Nat. Mater.* **2016**, *16*, 220–224.

(7) Feng, D.; Lei, T.; Lukatskaya, M. R.; Park, J.; Huang, Z.; Lee, M.; Shaw, L.; Chen, S.; Yakovenko, A. A.; Kulkarni, A.; Xiao,

J.; Fredrickson, K.; Tok, J. B.; Zou, X.; Cui, Y.; Bao, Z. Robust and Conductive Two-Dimensional Metal−organic Frameworks with Exceptionally High Volumetric and Areal Capacitance. *Nat. Energy* **2018**, *3*, 30–36.

(8) Alvaro, M.; Carbonell, E.; Ferrer, B.; Llabrés i Xamena, F. X.; Garcia, H. Semiconductor Behavior of a Metal-Organic Framework (MOF). *Chem. – A Eur. J.* **2007**, *13*, 5106–5112.

(9) Stassen, I.; Burtch, N.; Talin, A.; Falcaro, P.; Allendorf, M.; Ameloot, R. An Updated Roadmap for the Integration of Metal–organic Frameworks with Electronic Devices and Chemical Sensors. *Chem. Soc. Rev.* **2017**, *46*, 3185–3241.

(10) Wu, H. Bin; Lou, X. W. D. Metal-Organic Frameworks and Their Derived Materials for Electrochemical Energy Storage and Conversion: Promises and Challenges. *Sci. Adv.* **2017**, *3*, eaap9252.

(11) Zhou, J.; Wang, B. Emerging Crystalline Porous Materials as a Multifunctional Platform for Electrochemical Energy Storage. *Chem. Soc. Rev.* **2017**, *46*, 6927–6945.

(12) Mahmood, A.; Guo, W.; Tabassum, H.; Zou, R. Metal-Organic Framework-Based Nanomaterials for Electrocatalysis. *Adv. Energy Mater.* **2016**, *6*, 1600423.

(13) Fu, Y.; Sun, D.; Chen, Y.; Huang, R.; Ding, Z.; Fu, X.; Li, Z. An Amine-Functionalized Titanium Metal-Organic Framework Photocatalyst with Visible-Light-Induced Activity for CO_2 Reduction. *Angew. Chemie - Int. Ed.* **2012**, *51*, 3364–3367.

(14) Horiuchi, Y.; Toyao, T.; Saito, M.; Mochizuki, K.; Iwata, M.; Higashimura, H.; Anpo, M.; Matsuoka, M. Visible-Light-Promoted Photocatalytic Hydrogen Production by Using an Amino-Functionalized Ti(IV) Metal–Organic Framework. *J. Phys. Chem. C* **2012**, *116*, 20848–20853.

(15) Toyao, T.; Saito, M.; Horiuchi, Y.; Mochizuki, K.; Iwata, M.; Higashimura, H.; Matsuoka, M. Efficient Hydrogen Production and Photocatalytic Reduction of Nitrobenzene over a Visible-Light-Responsive Metal–organic Framework Photocatalyst. *Catal. Sci. Technol.* **2013**, *3*, 2092–2097.

(16) Dan-Hardi, M.; Serre, C.; Frot, T.; Rozes, L.; Maurin, G.; Sanchez, C.; Férey, G.; Maurín, G. A New Photoactive Highly Porous Titanium (IV) Dicarboxylate. *J. Am. Chem. Soc.* **2009**, *131*, 10857–10859.

(17) Nguyen, H. L.; Gándara, F.; Furukawa, H.; Doan, T. L. H.; Cordova, K. E.; Yaghi, O. M. A Titanium-Organic Framework as an Exemplar of Combining the Chemistry of Metal- and Covalent-Organic Frameworks. *J. Am. Chem. Soc.* **2016**, *138*, 4330–4333.

(18) Yuan, S.; Liu, T.-F.; Feng, D.; Tian, J.; Wang, K.; Qin, J.; Zhang, Q.; Chen, Y.-P.; Bosch, M.; Zou, L.; Teat, S. J.; Dalgarno, S. J.; Zhou, H.-C. A Single Crystalline Porphyrinic Titanium Metal–organic Framework. *Chem. Sci.* **2015**, *6*, 3926–3930.

(19) Yuan, S.; Qin, J.-S.; Xu, H.-Q.; Su, J.; Rossi, D.; Chen, Y.; Zhang, L.; Lollar, C.; Wang, Q.; Jiang, H.-L.; Son, D. H.; Xu, H.; Huang, Z.; Zou, X.; Zhou, H.-C. $[Ti_8Zr_2O_{12}(COO)_{16}]$ Cluster: An Ideal Inorganic Building Unit for Photoactive Metal–Organic Frameworks. *ACS Cent. Sci.* **2018**, *4*, 105–111.

(20) Chang, X.; Wang, T.; Gong, J. CO_2 Photo-Reduction: Insights into CO_2 Activation and Reaction on Surfaces of Photocatalysts. *Energy Environ. Sci.* **2016**, *9*, 2177–2196.

(21) Zhou, T.; Du, Y.; Borgna, A.; Hong, J.; Wang, Y.; Han, J.; Zhang, W.; Xu, R. Post-Synthesis Modification of a Metal-Organic Framework to Construct a Bifunctional Photocatalyst for Hydrogen Production. *Energy Environ. Sci.* **2013**, *6*, 3229–3234.

(22) Usov, P. M.; Ahrenholtz, S. R.; Maza, W. A.; Stratakes, B.; Epley, C. C.; Kessinger, M. C.; Zhu, J.; Morris, A. J. Cooperative Electrochemical Water Oxidation by Zr Nodes and Ni-Porphyrin Linkers of a PCN-224 MOF Thin Film. *J. Mater. Chem. A* **2016**, *4*, 16818–16823.

(23) Johnson, B. A.; Bhunia, A.; Fei, H.; Cohen, S. M.; Ott, S. Development of a UiO-Type Thin Film Electrocatalysis Platform with Redox-Active Linkers. *J. Am. Chem. Soc.* **2018**, *140*, 2985–2994.

(24) Celis-Salazar, P. J.; Epley, C. C.; Ahrenholtz, S. R.; Maza, W. A.; Usov, P. M.; Morris, A. J. Proton-Coupled Electron Transport in Anthraquinone-Based Zirconium Metal-Organic Frameworks. *Inorg. Chem.* **2017**, *56*, 13741–13747.

(25) Bueken, B.; Vermoortele, F.; Vanpoucke, D. E. P.; Reinsch, H.; Tsou, C.-C.; Valvekens, P.; De Baerdemaeker, T.; Ameloot, R.; Kirschhock, C. E. A.; Van Speybroeck, V.; Mayer, J. M.; De Vos, D. A Flexible Photoactive Titanium Metal-Organic Framework Based on a $[Ti^{IV}_3(\mu_3\text{-}O)(O)_2(COO)_6]$ Cluster. *Angew. Chemie Int. Ed.* **2015**, *54*, 13912–13917.

(26) Meyer, K.; Bashir, S.; Llorca, J.; Idriss, H.; Ranocchiari, M.; van Bokhoven, J. A. Photocatalyzed Hydrogen Evolution from Water by a Composite Catalyst of NH_2-MIL-125(Ti) and Surface Nickel(II) Species. *Chem. – A Eur. J.* **2016**, *22*, 13894–13899.

(27) Sandström, J. *Dynamic NMR Spectroscopy*; 1982.

(28) Sadakiyo, M.; Yamada, T.; Kitagawa, H. Proton Conductivity Control by Ion Substitution in a Highly Proton-Conductive Metal–Organic Framework. *J. Am. Chem. Soc.* **2014**, *136*, 13166–13169.

(29) Zhang, F.-M.; Dong, L.-Z.; Qin, J.-S.; Guan, W.; Liu, J.; Li, S.-L.; Lu, M.; Lan, Y.-Q.; Su, Z.-M.; Zhou, H.-C. Effect of Imidazole Arrangements on Proton-Conductivity in Metal–Organic Frameworks. *J. Am. Chem. Soc.* **2017**, *139*, 6183–6189.

(30) Lin, S.; Usov, P. M.; Morris, A. J. The Role of Redox Hopping in Metal–organic Framework Electrocatalysis. *Chem. Commun.* **2018**, *54*, 6965–6974.

(31) Li, A.-L.; Gao, Q.; Xu, J.; Bu, X.-H. Proton-Conductive Metal-Organic Frameworks: Recent Advances and Perspectives. *Coord. Chem. Rev.* **2017**, *344*, 54–82.

(32) Ling, S.; Slater, B. Dynamic Acidity in Defective UiO-66. *Chem. Sci.* **2016**, *7*, 4706–4712.

(33) Hajek, J.; Caratelli, C.; Demuynck, R.; De Wispelaere, K.; Vanduyfhuys, L.; Waroquier, M.; Van Speybroeck, V. On the Intrinsic Dynamic Nature of the Rigid UiO-66 Metal–organic Framework. *Chem. Sci.* **2018**, *9*, 2723–2732.

(34) Norby, T.; Widerøe, M.; Glöckner, R.; Larring, Y. Hydrogen in Oxides. *Dalt. Trans.* **2004**, No. 19, 3012–3018.

(35) Frot, T.; Cochet, S.; Laurent, G.; Sassoye, C.; Popall, M.; Sanchez, C.; Rozes, L. $Ti_8O_8(OOCR)_{16}$, a New Family of Titanium-Oxo Clusters: Potential NBUs for Reticular Chemistry. *Eur. J. Inorg. Chem.* **2010**, *8*, 5650–5659.

(36) Uetsuka, H.; Onishi, H.; Henderson, M. A.; White, J. M. Photoinduced Redox Reaction Coupled with Limited Electron Mobility at Metal Oxide Surface. *J. Phys. Chem. B* **2004**, *108*, 10621–10624.

Graphic entry for the Table of Contents (TOC):